

A quantitative ratiometric fluorescence Hddb-based MOF sensor and its on-site detection to the anthrax biomarker 2,6-dipicolinic acid

Xuan-Bo Chen,^a Cui-Xing Qi,^a Yu-Bin Xu,^b Hong Li,^c Ling Xu,^{c*} and Bing Liu^a

^a College of Chemistry and Chemical Engineering, Shaanxi Key Laboratory of Chemical Additives for Industry, Shaanxi University of Science and Technology, Xi'an 710021, Shaanxi Province, P. R. China.

^b Qidi Middle School attached to Northwestern Polytechnical University, Xianyang 712000, Shaanxi Province, P. R. China

^c Key Laboratory of Macromolecular Science of Shaanxi Province, Shaanxi Key Laboratory for Advanced Energy Devices, Shaanxi Engineering Laboratory for Advanced Energy Technology, School of Chemistry & Chemical Engineering, Shaanxi Normal University, Xi'an 710062, Shaanxi Province, P. R. China

Table S1. The structural determination and refinement data for Eu-Hddb.

Empirical formula	C ₂₂ H ₁₅ EuO ₁₀
Color and Habit	Yellow platelet
Crystal Size (mm ³)	0.40 × 0.10 × 0.10
Crystal system	triclinic
Space group	P-1
<i>a</i> (Å)	9.839(3)
<i>b</i> (Å)	10.617(3)
<i>c</i> (Å)	10.851(3)
$\alpha/^\circ$	82.065(10)
$\beta/^\circ$	86.784(10)
$\gamma/^\circ$	87.139(11)
<i>V</i> /Å ³	1119.9(6)
<i>Z</i>	2
<i>Fw</i>	591.30
<i>D</i> _{calcd} (Mgm ⁻³)	1.754
μ (mm ⁻¹)	2.855
<i>F</i> (000)	580.0
2 <i>θ</i> (°)	7.106 to 50.046
Reflections measured	11892
Independent reflections	3926 [<i>R</i> _{int} = 0.0543, <i>R</i> _{sigma} = 0.0571]
<i>S</i>	1.053
Final <i>R</i> ₁ , <i>wR</i> ₂ indices (obs.)	<i>R</i> ₁ = 0.0542, <i>wR</i> ₂ = 0.1474
<i>R</i> ₁ , <i>wR</i> ₂ indices (all)	<i>R</i> ₁ = 0.0612, <i>wR</i> ₂ = 0.1526

$$R_1 = (\sum ||F_o|| - |F_c|) / \sum |F_o|. wR_2 = [\sum (w(F_o^2 - F_c^2)^2) / \sum (w |F_o|^2)]^{1/2}$$

Table S2. Selected bond distances (Å) and bond angles (°) of Eu-Hddb.

Eu1-O12=2.357(6)	Eu1-O18 ³ =2.437(6)
Eu1-O1W=2.381(6)	Eu1-O15 ⁴ =2.446(6)
Eu1-O14 ¹ =2.386(5)	Eu1-O17 ³ =2.518(6)
Eu1-O11 ² =2.391(6)	Eu1-O16 ⁴ =2.532(6))
O12-Eu1-O1W=109.3(2)	O18 ³ -Eu1-O15 ⁴ =122.4(2)
O12-Eu1-O14 ¹ =74.1(2)	O12-Eu1-O17 ³ =112.4(2)
O1W-Eu1-O14 ¹ =75.0(2)	O1W -Eu1-O17 ³ =116.4(2)
O12-Eu1-O11 ² =95.2(2)	O14 ¹ -Eu1-O17 ³ =73.0(2)
O1W-Eu1-O11 ² =144.5(2)	O11 ² -Eu1-O17 ³ =74.5(2)
O14 ¹ -Eu1-O11 ² =138.2(2)	O18 ³ -Eu1-O17 ³ =52.69(19)
O12-Eu1-O18 ³ =165.0(2)	O15 ⁴ -Eu1-O17 ³ =162.5(2)
O1W-Eu1-O18 ³ =79.8(2)	O12-Eu1-O16 ⁴ =123.13(19)
O14 ¹ -Eu1-O18 ³ =97.6(2)	O1W -Eu1-O16 ⁴ =70.7(2)
O11 ² -Eu1-O18 ³ =82.7(2)	O14 ¹ -Eu1-O16 ⁴ =145.1(2)
O12-Eu1-O15 ⁴ =72.2(2)	O11 ² -Eu1-O16 ⁴ =74.4(2)
O1W-Eu1-O15 ⁴ =75.6(2)	O18 ³ -Eu1-O16 ⁴ =70.69(19)
O14 ¹ -Eu1-O15 ⁴ =124.0(2)	O15 ⁴ -Eu1-O16 ⁴ =52.1(2)
O11 ² -Eu1-O15 ⁴ =88.4(2)	O17 ³ -Eu1- O16 ⁴ =117.59(19)

Symmetry codes: ¹ -x, -1-y, -z; ² -x, -y, -z; ³ -x, -y, -1-z; ⁴ -1-x, -y, -1-z

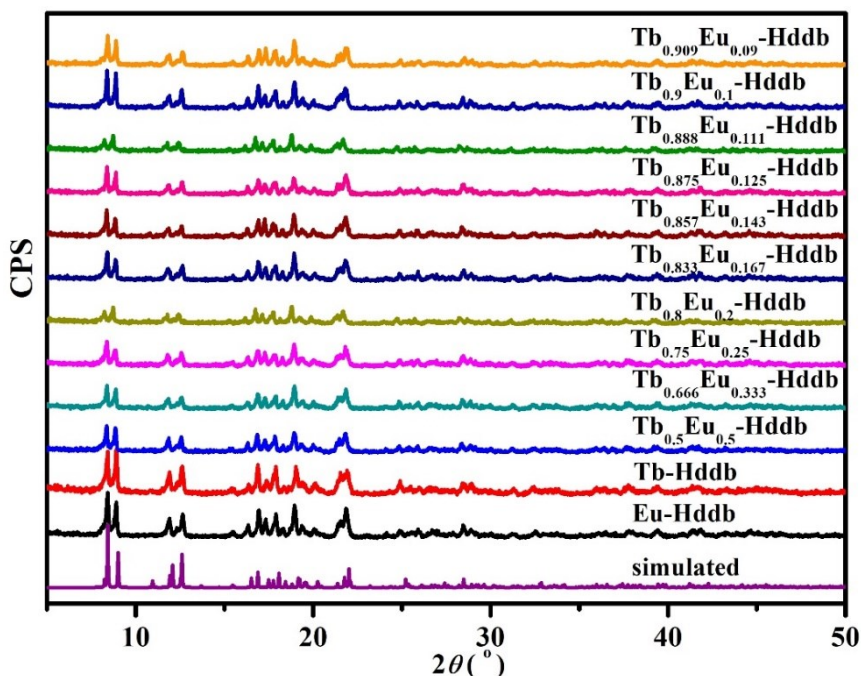


Fig. S1. Experimental PXRD patterns of Eu-Hddb, Tb-Hddb, and $\text{Tb}_x\text{Eu}_{1-x}\text{-Hddb}$ ($\text{Tb}^{3+}:\text{Eu}^{3+}$ molar ratios being 10:1, 9:1, 8:1, 7:1, 6:1, 5:1, 4:1, 3:1, 2:1 and 1:1) with simulated PXRD pattern from single crystal data of Eu-Hddb as comparison.

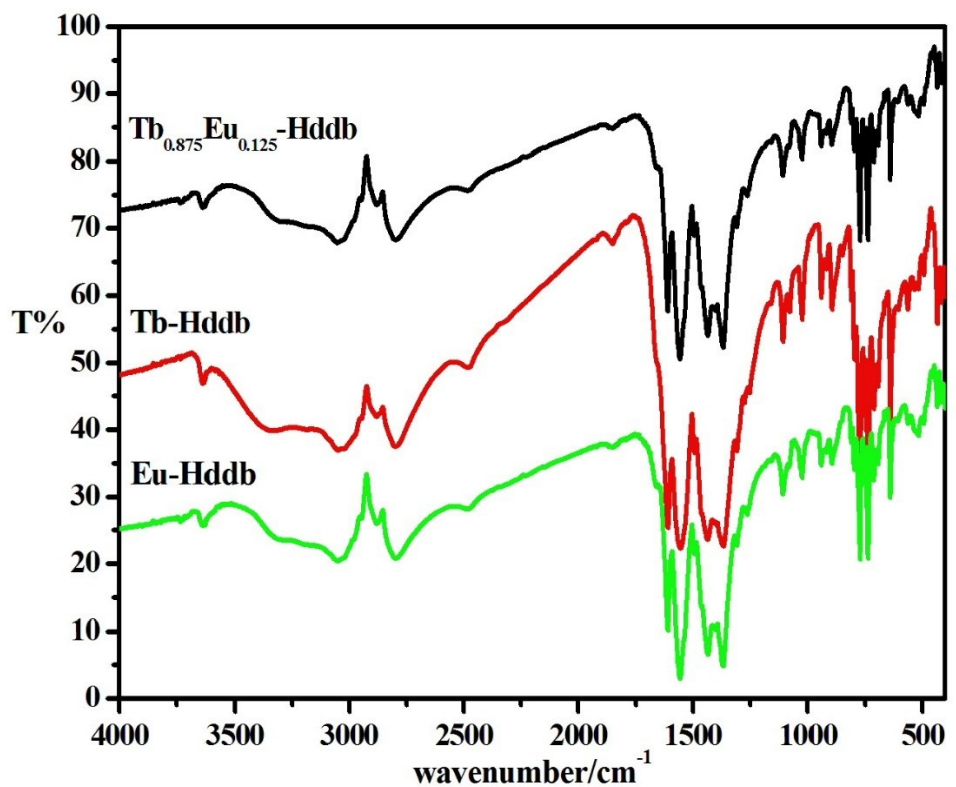


Fig. S2. FT-IR spectra of Eu-Hddb, Tb-Hddb, Tb_{0.875}Eu_{0.125}-Hddb.

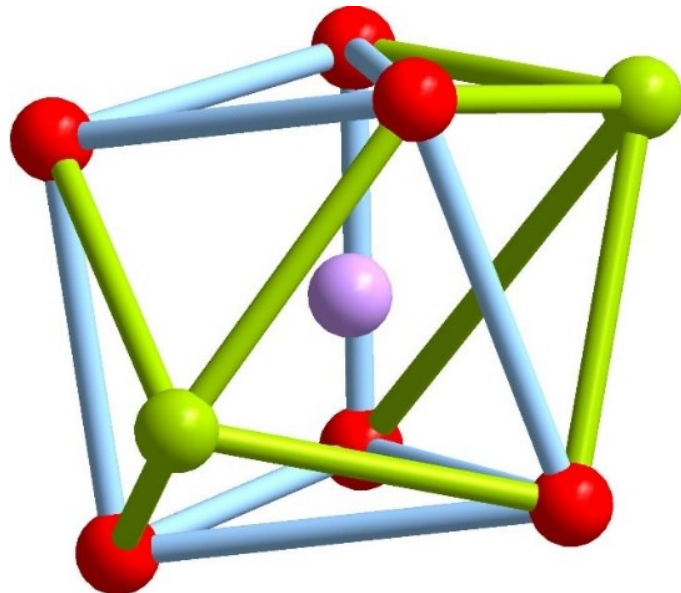
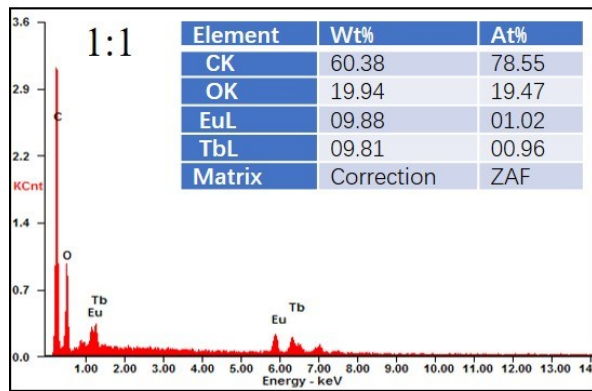
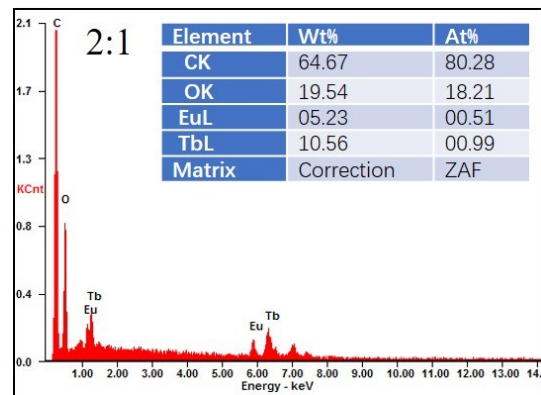


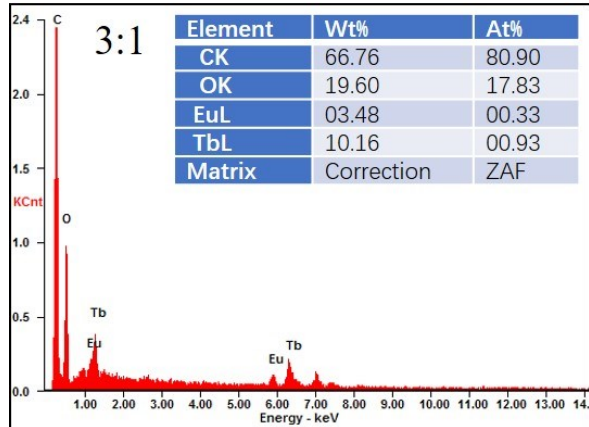
Fig. S3. The bi-capped trigonal prism of the eight-coordinated Eu(III) center in Eu-Hddb.



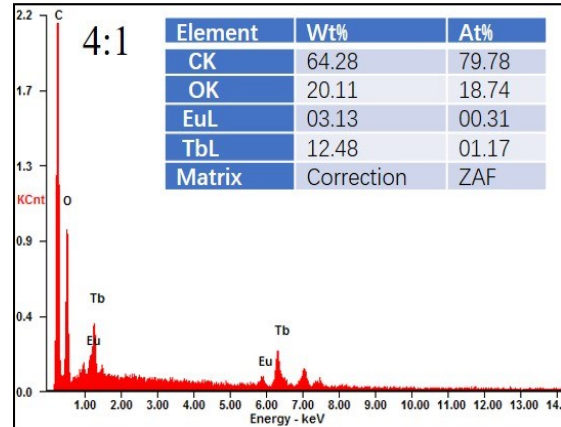
(a)



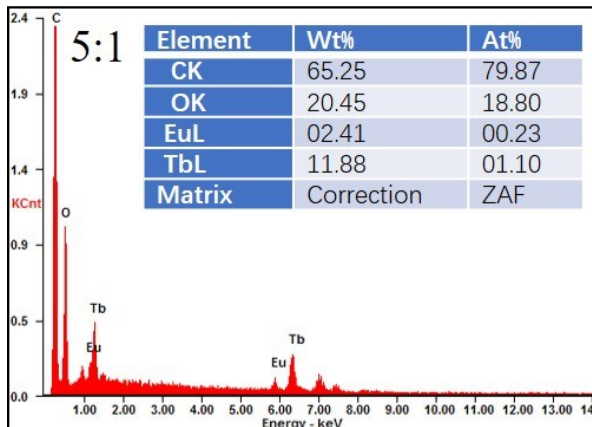
(b)



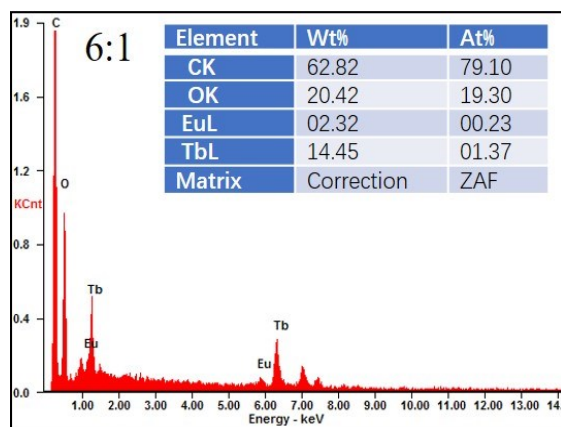
(c)



(d)



(e)



(f)

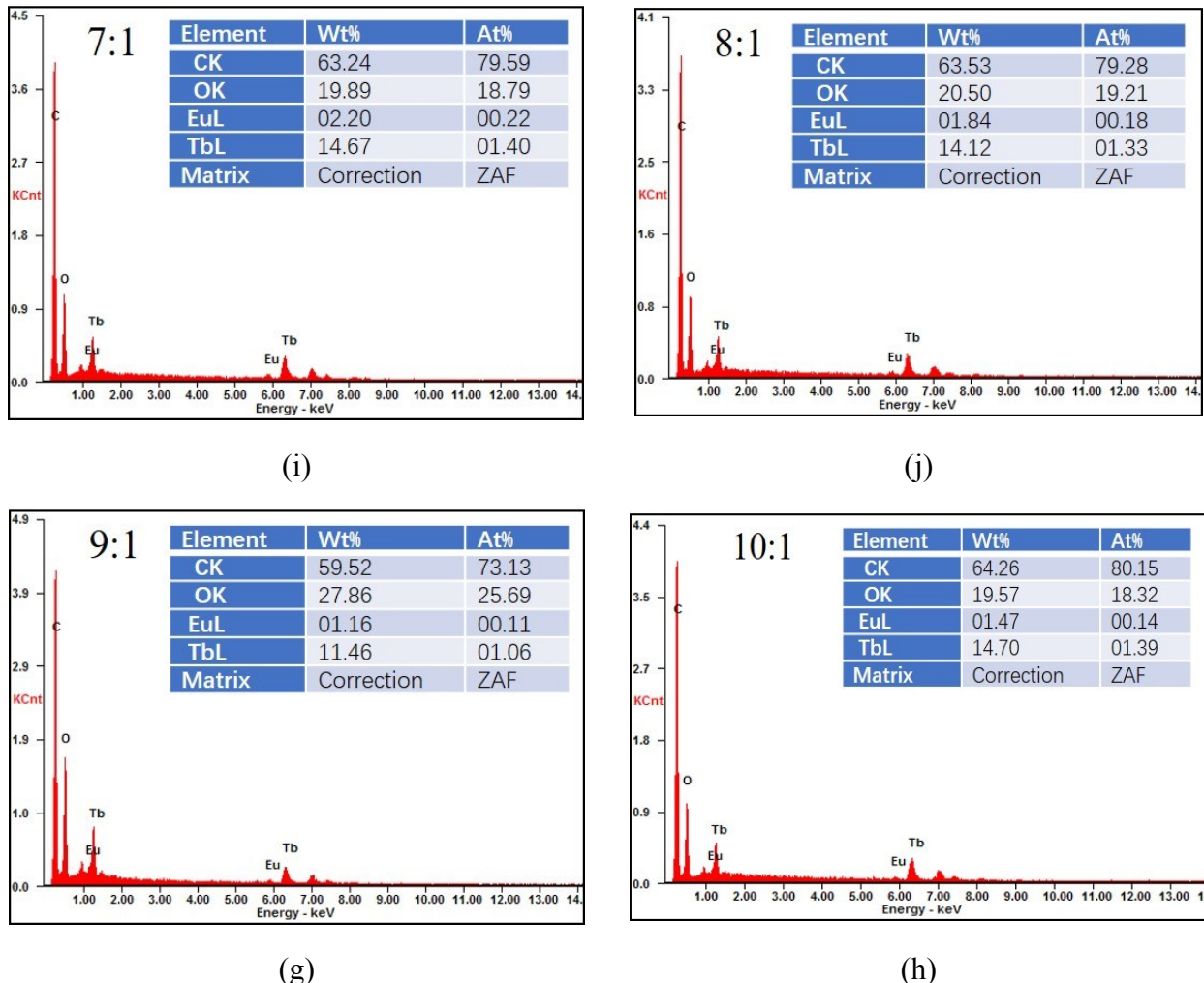


Fig. S4. The elemental content ratios of Tb^{3+} and Eu^{3+} in $\text{Tb}_x\text{Eu}_{1-x}\text{-Hddb}$ characterized by EDS.

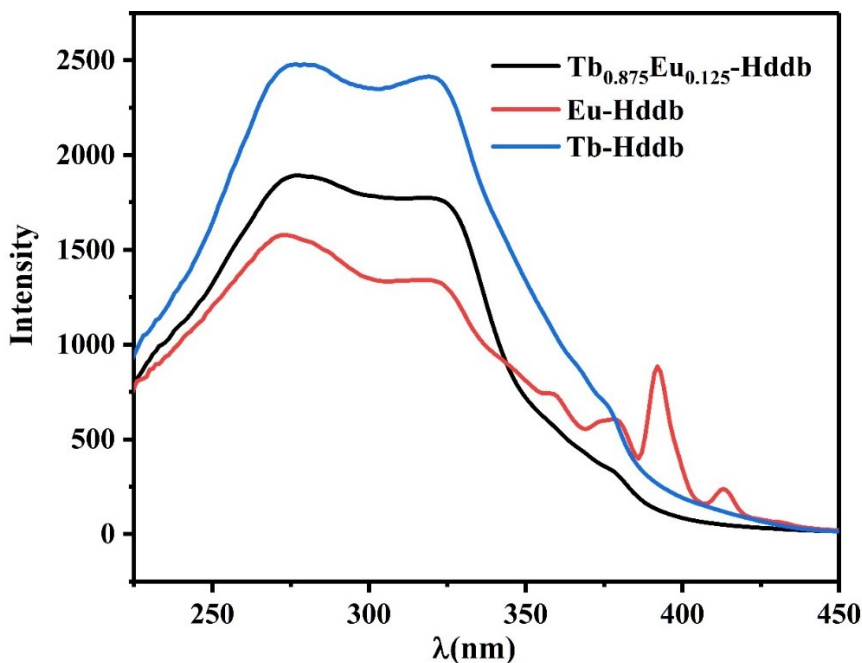


Fig. S5. The excitation spectra of Eu-Hddb, Tb-Hddb, and $\text{Tb}_{0.875}\text{Eu}_{0.125}\text{-Hddb}$ excited at 270 nm at ambient temperature.

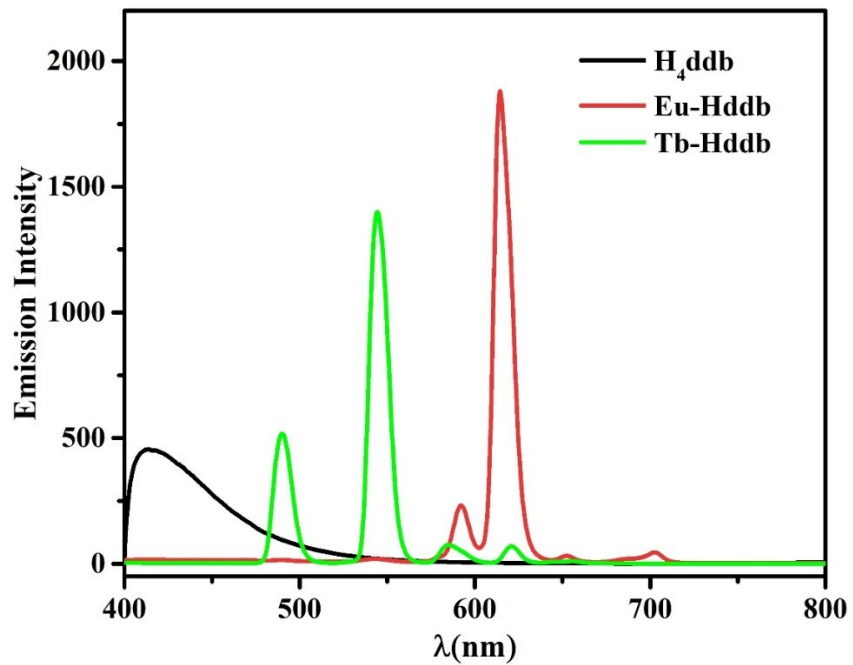


Fig. S6. The emission spectra of Tb-Hddb, Eu-Hddb, and free $H_4\text{ddb}$ excited at 270 nm at ambient temperature.

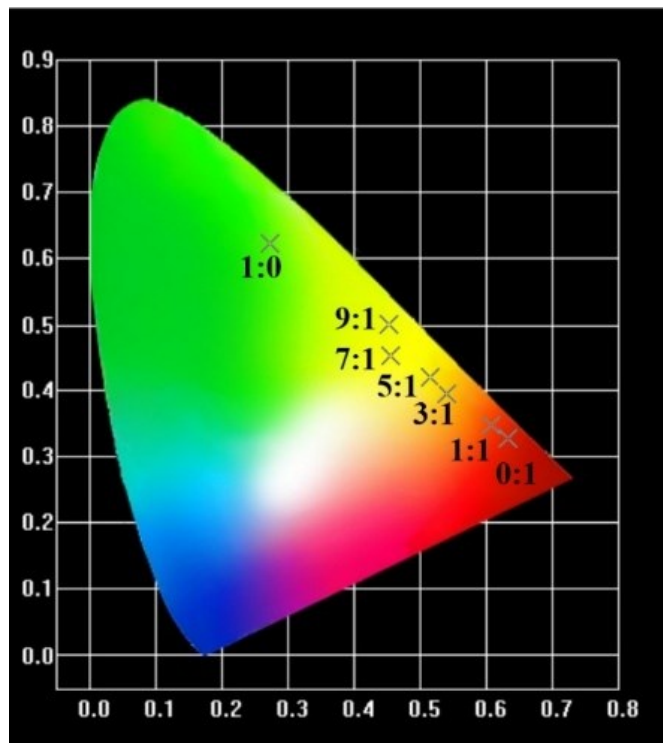


Fig. S7. The CIE 1931 chromaticity diagram of Tb-Hddb (1:0), Eu-Hddb (0:1), and $Tb_xEu_{1-x}\text{-Hddb}$ (only a part of them are listed for clarity).

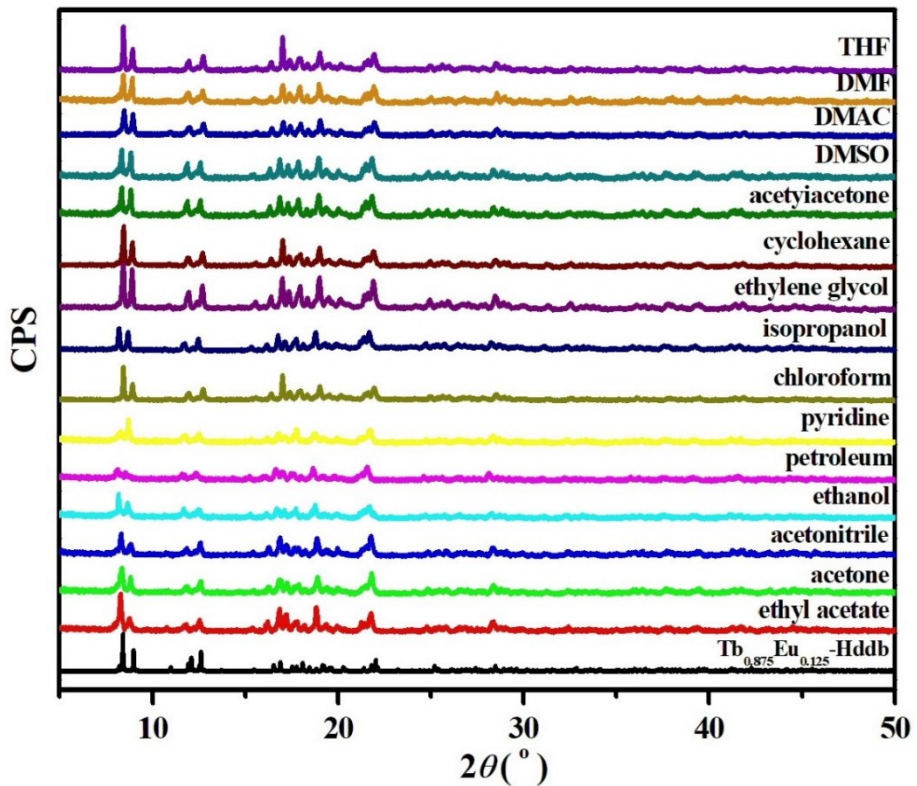


Fig. S8. Experimental PXRD patterns of $\text{Tb}_{0.875}\text{Eu}_{0.125}$ -Hddb immersed in fifteen organic solvents for 3h compared with $\text{Tb}_{0.875}\text{Eu}_{0.125}$ -Hddb as comparison.

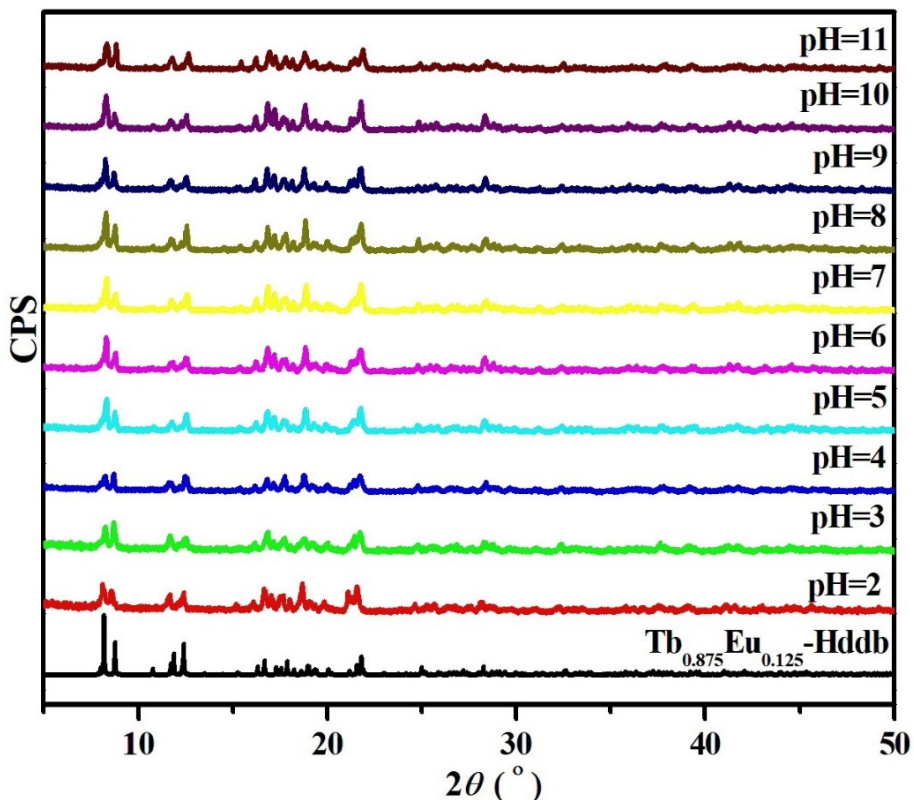


Fig. S9. Experimental PXRD patterns of $\text{Tb}_{0.875}\text{Eu}_{0.125}$ -Hddb immersed in water for 48h with HCl or NaOH solutions adjusting pH =2-11 compared to the one of $\text{Tb}_{0.875}\text{Eu}_{0.125}$ -Hddb.

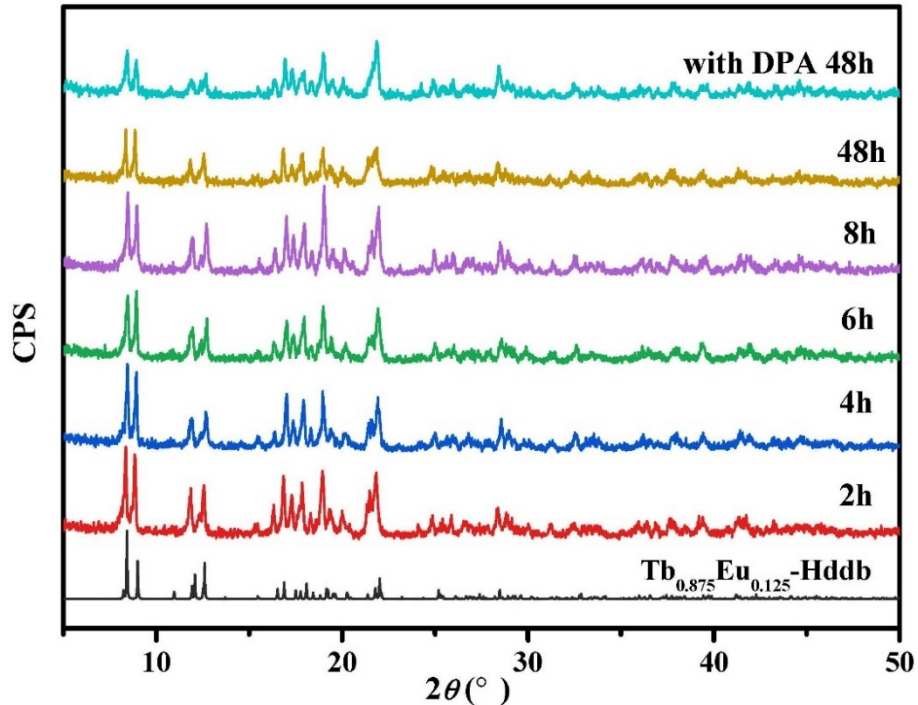


Fig. S10. Experimental PXRD patterns of $\text{Tb}_{0.875}\text{Eu}_{0.125}\text{-Hddb}$ immersed in HEPES buffer solution (pH = 7.35) for 1, 2, 3, 4 and 48 h without or with DPA compared to the one of $\text{Tb}_{0.875}\text{Eu}_{0.125}\text{-Hddb}$.

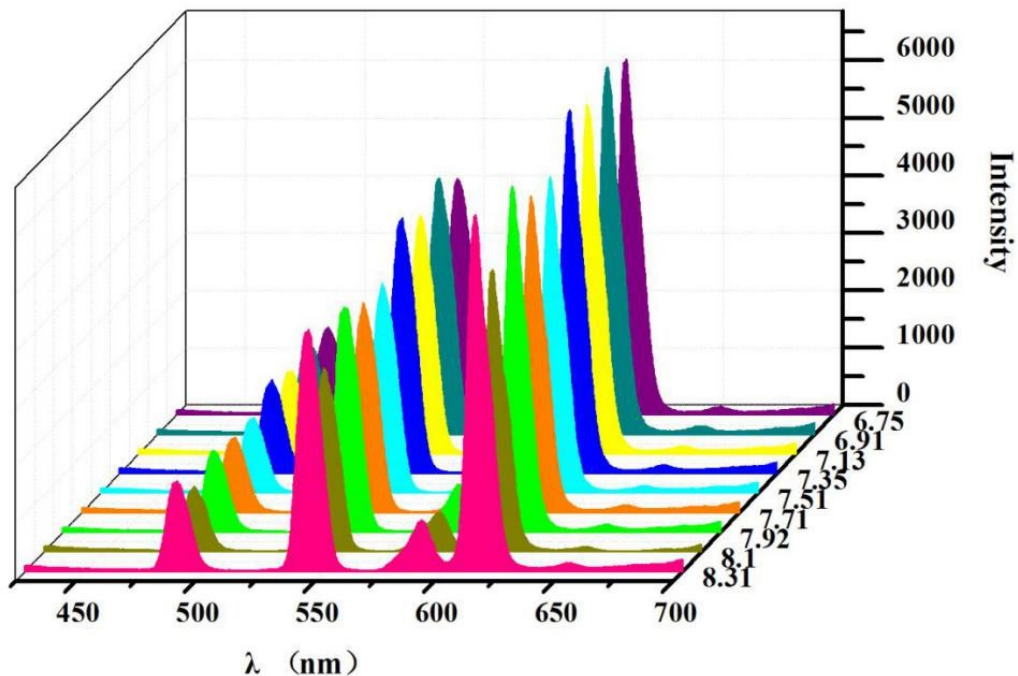


Fig. S11. The emission spectra of $\text{Tb}_{0.875}\text{Eu}_{0.125}\text{-Hddb}$ HEPES suspensions excited at 270 nm with pH ranging 6.75-8.31 without DPA added at ambient temperature.

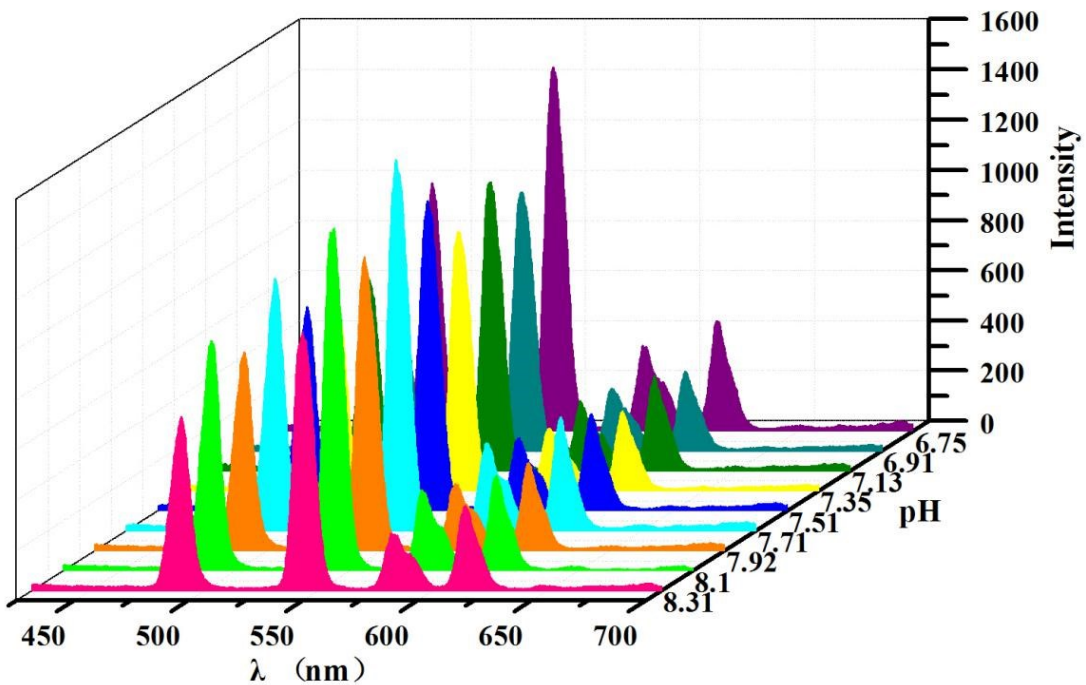


Fig. S12. The emission spectra of $\text{Tb}_{0.875}\text{Eu}_{0.125}$ -Hddb HEPES suspensions excited at 270 nm with pH ranging 6.75-8.31 with DPA added at ambient temperature.

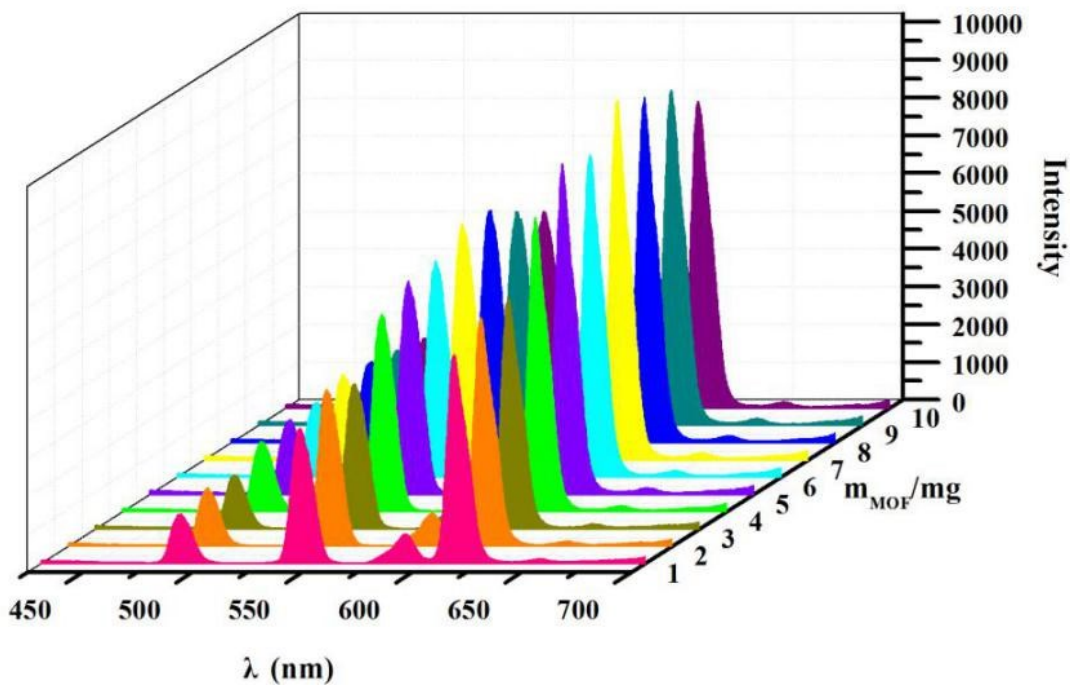


Fig. S13. The emission spectra of $\text{Tb}_{0.875}\text{Eu}_{0.125}$ -Hddb HEPES suspensions excited at 270 nm depending on the dosage of $\text{Tb}_{0.875}\text{Eu}_{0.125}$ -Hddb in 1-10 mg without DPA added at ambient temperature.

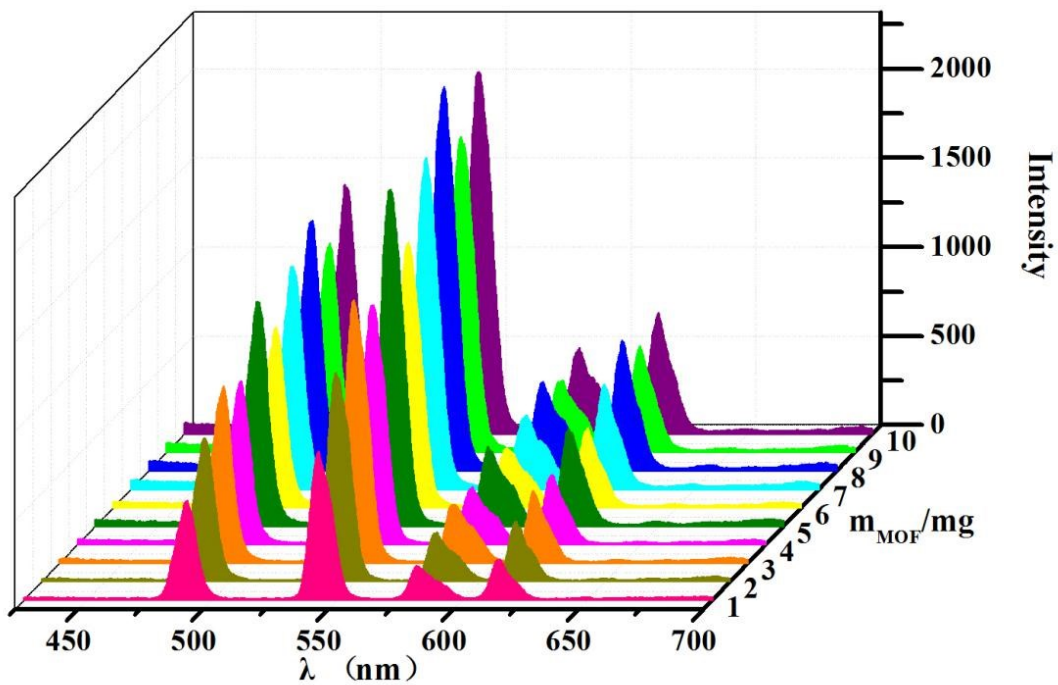


Fig. S14. The emission spectra of $\text{Tb}_{0.875}\text{Eu}_{0.125}$ -Hddb HEPES suspensions excited at 270 nm depending on the dosage of $\text{Tb}_{0.875}\text{Eu}_{0.125}$ -Hddb in 1-10 mg with DPA added at ambient temperature.

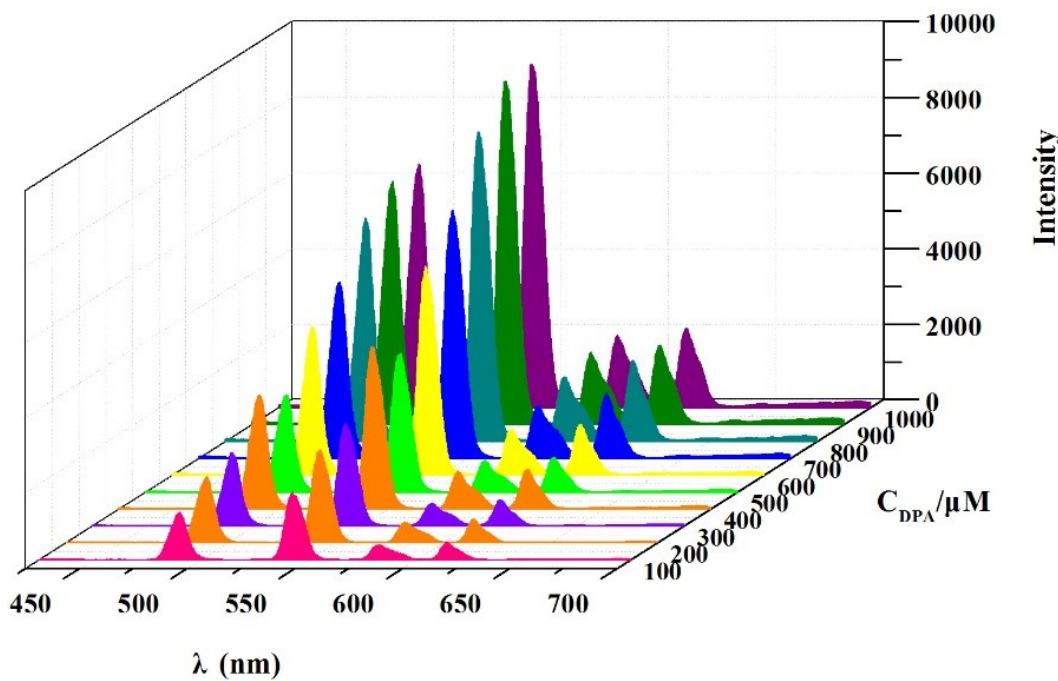


Fig. S15. The emission spectra of $\text{Tb}_{0.875}\text{Eu}_{0.125}$ -Hddb HEPES suspensions depending on C_{DPA} in 100-1000 μM excited at 270 nm at ambient temperature.

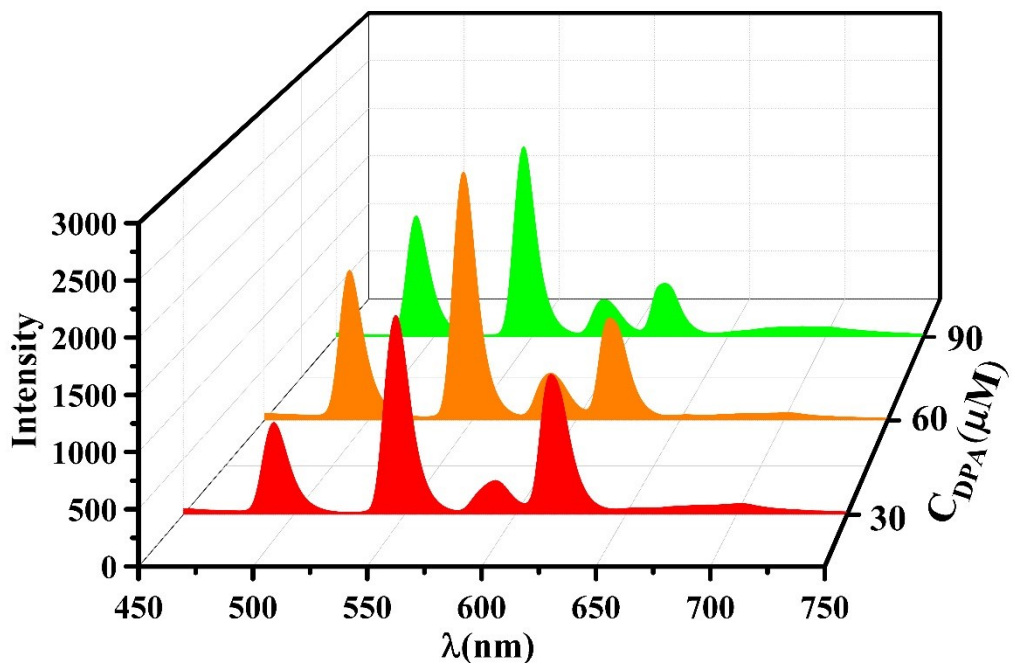


Fig. 16. The emission spectra of $Tb_{0.875}Eu_{0.125}$ -Hddb HEPES suspensions in human serum with $C_{DPA} = 30, 60$ and $90 \mu M$ excited at 270 nm at ambient temperature.

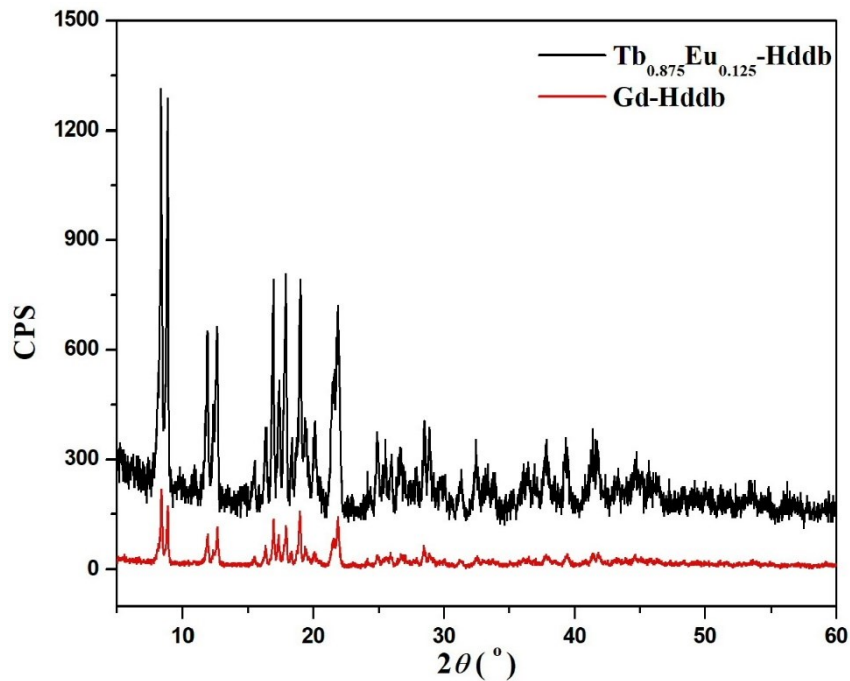


Fig. S17. An experimental PXRD pattern comparison of Gd-Hddb and $Tb_{0.875}Eu_{0.125}$ -Hddb.

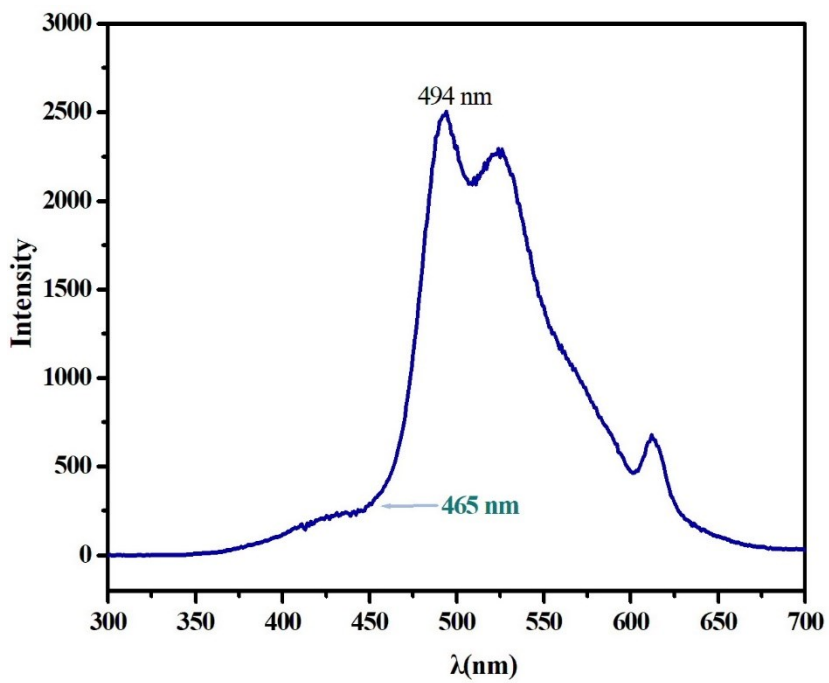


Fig. S18. Low-temperature phosphorescence spectrum of Gd-Hddb under 270 nm excitation at 77 K.

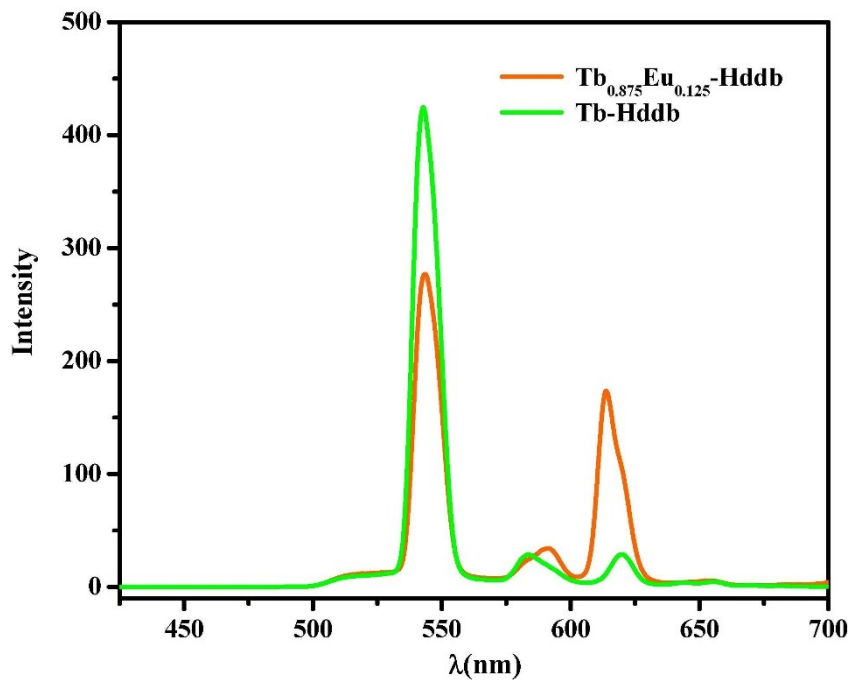


Fig. S19. The emission spectra of $Tb_{0.875}Eu_{0.125}\text{-Hddb}$ and $Tb\text{-Hddb}$ excited at 488 nm.

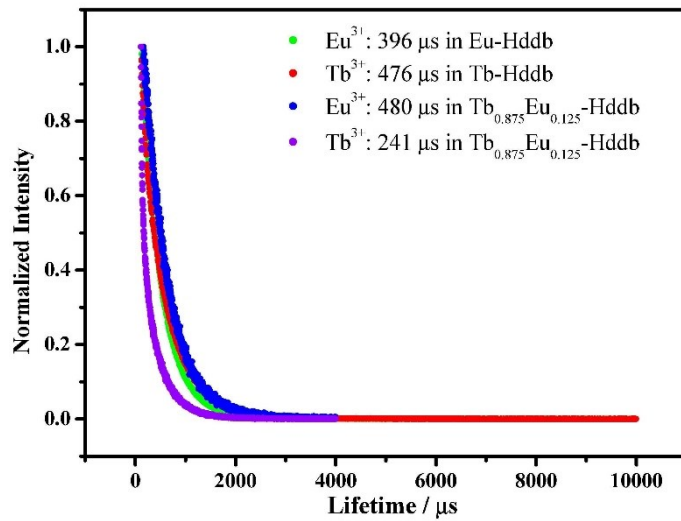


Fig. S20. The fluorescence lifetimes of Eu³⁺ and Tb³⁺ in Eu-Hddb, Tb-Hddb, and Tb_{0.875}Eu_{0.125}-Hddb.

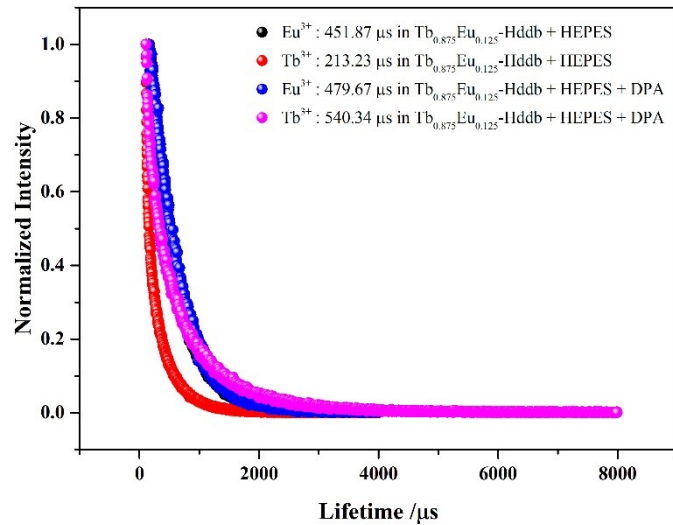


Fig. S21. The fluorescence lifetimes of Eu³⁺ and Tb³⁺ in Tb_{0.875}Eu_{0.125}-Hddb after DPA added.